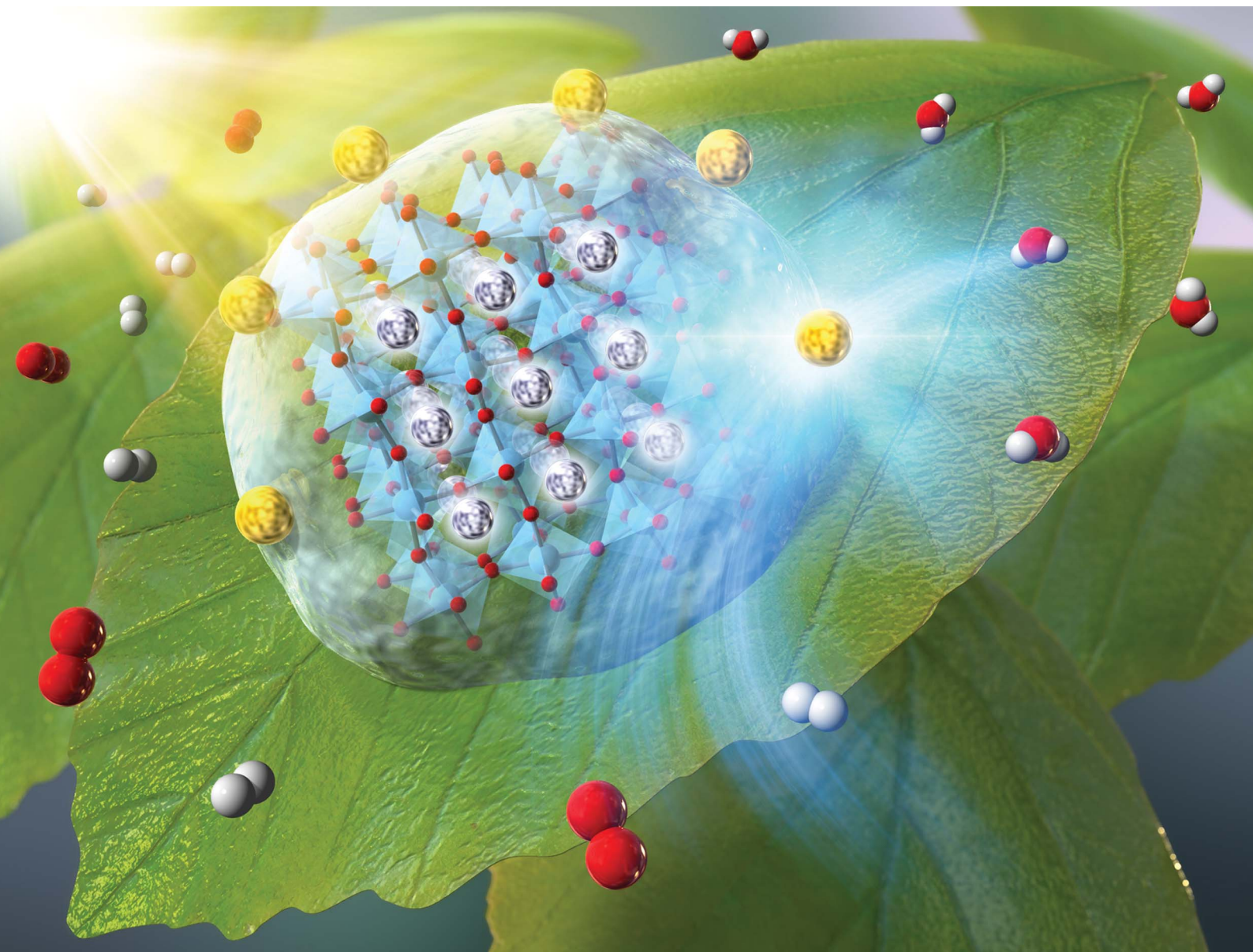


Chemical Science

Volume 11
Number 9
7 March 2020
Pages 2305–2574

rsc.li/chemical-science



ISSN 2041-6539

EDGE ARTICLE

Akihiko Kudo *et al.*

Solar water splitting over $\text{Rh}_{0.5}\text{Cr}_{1.5}\text{O}_3$ -loaded AgTaO_3 of a valence-band-controlled metal oxide photocatalyst

Cite this: *Chem. Sci.*, 2020, **11**, 2330

All publication charges for this article have been paid for by the Royal Society of Chemistry

Received 21st November 2019

Accepted 28th January 2020

DOI: 10.1039/c9sc05909a

rsc.li/chemical-science

Solar water splitting over $\text{Rh}_{0.5}\text{Cr}_{1.5}\text{O}_3$ -loaded AgTaO_3 of a valence-band-controlled metal oxide photocatalyst†

Kenta Watanabe,^a Akihito Iwase^{ab} and Akihiko Kudo^{ab*}

Improvement of water splitting performance of AgTaO_3 (BG 3.4 eV) of a valence-band-controlled photocatalyst was examined. Survey of cocatalysts revealed that a $\text{Rh}_{0.5}\text{Cr}_{1.5}\text{O}_3$ cocatalyst was much more effective than Cr_2O_3 , RuO_2 , NiO and Pt for water splitting into H_2 and O_2 in a stoichiometric amount. The optimum loading amount of the $\text{Rh}_{0.5}\text{Cr}_{1.5}\text{O}_3$ cocatalyst was 0.2 wt%. The apparent quantum yield (AQY) at 340 nm of the optimized $\text{Rh}_{0.5}\text{Cr}_{1.5}\text{O}_3$ (0.2 wt%)/ AgTaO_3 photocatalyst reached to about 40%. $\text{Rh}_{0.5}\text{Cr}_{1.5}\text{O}_3$ (0.2 wt%)/ AgTaO_3 gave a solar to hydrogen conversion efficiency (STH) of 0.13% for photocatalytic water splitting under simulated sunlight irradiation. Bubbles of gasses evolved by the solar water splitting were visually observed under atmospheric pressure at room temperature.

Introduction

Photocatalytic solar water splitting is an important reaction because it has the potential for solving resources, energy and environmental issues. Hence, many researchers have aimed to develop water splitting systems of a one-step photoexcitation type and a two-step photoexcitation type (Z-scheme) with visible-light-driven powdered photocatalysts.^{1–6} The simplicity of the one-step photoexcitation type will be an advantage in practical use. Domen and co-workers have reported that (oxy)nitride and oxysulfide photocatalysts such as GaN-ZnO ,^{7,8} $\text{ZnGeN}_2\text{-ZnO}$,^{9,10} $\text{LaMg}_{1/3}\text{Ta}_{2/3}\text{O}_2\text{N}$,^{11–13} TaON ,¹⁴ CaTaO_2N ,¹⁵ Ta_3N_5 (ref. 16) and $\text{Y}_2\text{Ti}_2\text{O}_5\text{S}_2$ (ref. 17) show activities for one-step photoexcitation type water splitting under visible light irradiation. We have also reported that Rh,Sb-codoped SrTiO_3 of a metal oxide photocatalyst shows the water splitting activity under visible light irradiation by loading of an IrO_2 cocatalyst.¹⁸ Although above visible-light-responsive photocatalysts split water under sunlight irradiation, their solar energy conversion efficiencies (solar to hydrogen conversion efficiency, STH) do not reach the level for practical use due to low apparent quantum yields (AQY). In terms of the high AQY, NiO-loaded La-doped NaTaO_3 (ref. 19) (BG 4.1 eV), $\text{Rh}_{0.5}\text{Cr}_{1.5}\text{O}_3$ -loaded Zn,Ca-codoped Ga_2O_3 (ref. 20) (BG 4.6 eV) and MoO_y ,RhCrO_x-coloaded Al-doped SrTiO_3 (ref. 21) (BG 3.2 eV) show the AQYs of 56% at 270 nm, 71% at 254 nm and 69% at

365 nm, for photocatalytic water splitting under UV irradiation, respectively. However, only Al-doped SrTiO_3 can respond to sunlight ($\lambda > 300$ nm) with STH of 0.4%.²² Thus, the development of sunlight-driven photocatalysts with one-step photoexcitation for water splitting is an important research topic.

We have reported that a AgTaO_3 photocatalyst (BG 3.4 eV) shows water splitting activity under UV irradiation by loading of a NiO cocatalyst.²³ The characteristics of AgTaO_3 is the valence band maximums formed by Ag 4d orbitals which are located above the bands formed by O 2p orbitals, and hence the band gap of AgTaO_3 is relatively narrow among the metal oxides containing Ta. AgTaO_3 is expected to respond to sunlight judging from the band gap of 3.4 eV, while the water splitting under sunlight irradiation has not been achieved yet. Moreover, the crystal structure of perovskite for AgTaO_3 is the same as that for SrTiO_3 and NaTaO_3 photocatalysts with high activities for water splitting. These backgrounds motivate us to investigate solar water splitting using the AgTaO_3 photocatalyst.

A cocatalyst is one of the most effective factors for improvement of the photocatalytic activity. Actually, the water splitting activity of AgTaO_3 is drastically improved by loading of a NiO cocatalyst which is widely used in water splitting over metal oxides.²³ Recently, $\text{Rh}_{0.5}\text{Cr}_{1.5}\text{O}_3$ has also arisen as a potential candidate cocatalyst for water splitting over metal oxides.^{20,21} In the present study, we investigated the loading effect of various cocatalysts on water splitting over AgTaO_3 . Solar water splitting was also demonstrated using the AgTaO_3 with the optimized cocatalyst.

Experimental

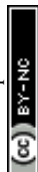
Preparation of photocatalysts

AgTaO_3 was synthesized by a solid-state reaction using Ag_2O (Kanto Chemical; 99.0%) and Ta_2O_5 (Rare Metallic; 99.99%) as

^aDepartment of Applied Chemistry, Faculty of Science, Tokyo University of Science, 1-3 Kagurazaka, Shinjuku-ku, Tokyo 162-8601, Japan. E-mail: a-kudo@rs.tus.ac.jp

^bPhotocatalysis International Research Center, Research Institute for Science and Technology, Tokyo University of Science, 2641 Yamazaki, Noda-shi, Chiba-ken 278-8510, Japan

† Electronic supplementary information (ESI) available. See DOI: 10.1039/c9sc05909a



starting materials. The starting materials were mixed in an alumina mortar in a ratio of Ag : Ta = 1 + x : 1 (x = 0, 0.03, 0.05, 0.07). The mixture was calcined in air at 1173–1373 K for 5–20 h in an alumina crucible. The calcined materials were washed with 1 mol L⁻¹ of an aqueous HNO₃ solution in ultrasonication for 1 h in order to remove Ag metals deposited on the surface of AgTaO₃.

A Pt cocatalyst was loaded *in situ* by a photodeposition method using an aqueous H₂PtCl₆ (Tanaka Kikinzoku; 37.7 wt% as Pt) solution. NiO,²³ RuO₂ (ref. 24) and Cr₂O₃ (ref. 25) of cocatalysts were loaded on AgTaO₃ photocatalysts by an impregnation method using Ni(NO₃)₂·6H₂O (Wako Pure Chemical; 98.0%), Ru₃(CO)₁₂ (Aldrich; 99%), Cr(NO₃)₃·9H₂O (Kanto Chemical; 98.0–103.0%). AgTaO₃ powder was suspended in aqueous solutions dissolving Ni(NO₃)₂ or Cr(NO₃)₃, and an acetone solution dissolving Ru₃(CO)₁₂ in porcelain crucibles. The AgTaO₃-suspended solutions were dried up on a water bath and subsequently calcined in an electric furnace with conditions of 543 K – 1 h for NiO, 673 K – 2 h for RuO₂ and 623 K – 1 h for Cr₂O₃. Rh_{0.5}Cr_{1.5}O₃ (ref. 25) cocatalyst was loaded by a simple impregnation method using Cr(NO₃)₃·9H₂O and Rh(NO₃)₃ (Kanto Chemical; >80.0% as anhydrous). AgTaO₃-suspended aqueous solution containing both Rh(NO₃)₃ and Cr(NO₃)₃ was dried up and subsequently calcined at 623 K for 1 h. It is reported that Rh_{0.5}Cr_{1.5}O₃ of a mixed oxide is naturally formed on a photocatalyst by this process.²⁶ The loading amount of Rh_{0.5}Cr_{1.5}O₃ was controlled by adjusting the amount of starting materials.

Characterization

The crystal structure of the synthesized AgTaO₃ was identified by powder X-ray diffraction (Rigaku; MiniFlex600). The elemental composition of the synthesized AgTaO₃ was measured by an X-ray fluorescence spectrometer (Rigaku; NEX DE). A Diffuse reflectance spectrum was measured using a UV-vis-NIR spectrometer with an integrating sphere (Jasco; UbeatV-570) and was converted from reflection to absorbance mode by the Kubelka–Munk method. Morphologies of photocatalyst particles and Rh_{0.5}Cr_{1.5}O₃-cocatalysts were observed using a scanning electron microscope (JEOL; JSM-7400F) and a transmission electron microscope (JEOL; JEM-2100F). A chemical state of Rh in Rh_{0.5}Cr_{1.5}O₃-loaded AgTaO₃ was analyzed using an X-ray photoelectron spectroscopy (JEOL; JPS-9010MC).

Photocatalytic reaction

Photocatalytic water splitting was carried out in a gas-closed-circulation system. Photocatalyst powder (0.3 g) was dispersed in distilled water (120 mL) in a top-irradiation cell with a Pyrex window. A 300 W Xe-arc lamp (PerkinElmer; Cermex-PE300BF) and a solar simulator (Asahi spectra; HAL-320) were employed as a light source. An inner-irradiation reaction cell made of quartz equipped with a 400 W high-pressure Hg lamp (SEN; HL400EH-5) was also used for photocatalytic water splitting in order to compare with the activity of NiO/NaTaO₃:La.¹⁹ Amounts of evolved H₂ and O₂ gases were determined with a gas

chromatograph (Shimadzu; GC-8A, MS-5A, Ar carrier gas, TCD). Turnover number (TON) of the amount of reacted electrons/holes to the molar quantity of AgTaO₃ was estimated using the eqn (1).

$$\begin{aligned} [\text{TON}] &= [\text{the molar quantity of reacted electrons}] / \\ &\quad [\text{the molar quantity of AgTaO}_3] \\ &= [(\text{the amount of evolved H}_2) \times 2/\text{mol}] / \\ &\quad [\text{the molar quantity of AgTaO}_3/\text{mol}] \end{aligned} \quad (1)$$

Apparent quantum yields (AQY) were measured using a 300 W Xe-arc lamp (Asahi Spectra; MAX-302) with band-pass filters (Asahi Spectra). The photon flux of the monochromatic light through the long-pass filters was measured using a silicon diode head (OPHIR; PD300-UV head and NOVA display). An AQY and a solar to hydrogen conversion efficiency (STH) were estimated using the following eqn (2) and (3).

$$\begin{aligned} [\text{AQY}\%] &= 100 \times [\text{the number of reacted electrons or holes}] / \\ &\quad [\text{the number of incident photons}] = 100 \times \\ &\quad [(\text{the number of evolved H}_2 \text{ molecules}) \times 2] / \\ &\quad [\text{the number of incident photons}] \end{aligned} \quad (2)$$

$$\begin{aligned} [\text{STH}\%] &= 100 \times [(\Delta G^0(\text{H}_2\text{O})/\text{kJ mol}^{-1}) \\ &\quad \times [\text{rate of H}_2 \text{ evolution}/\mu\text{mol h}^{-1}]] / [\text{irradiation time/s}] \\ &\quad \times [\text{solar energy (AM1.5G)/mW cm}^{-2}] \\ &\quad \times [\text{irradiation area/cm}^2] = (237 \\ &\quad \times [\text{rate of H}_2 \text{ evolution}/\mu\text{mol h}^{-1}]) / \\ &\quad (3600 \times 100 \times 25) \times 100 \end{aligned} \quad (3)$$

Results and discussion

XRD measurement confirmed that trigonal AgTaO₃ with a perovskite structure was successfully synthesized in a single phase as previously reported (Fig. S1†).²³ The peaks due to metallic Ag were not observed in XRD patterns of AgTaO₃ both before and after washing with an aqueous HNO₃ solution. However, the absorption due to the surface plasmonic resonance of Ag was observed in diffuse reflectance spectra of the AgTaO₃ before and after the washing (Fig. S2†). The absorption due to the surface plasmonic resonance after the washing was a little bit smaller than that before the washing. Therefore, metallic Ag on the surface would be removed by the washing but the amount of removed Ag was quite small. Actually, atomic ratios of Ag to Ta in the AgTaO₃ after the washing were calculated to be 1.00 and 0.99 from XPS and XRF measurements, respectively. These results indicate that the ratios of Ag to Ta on the surface and in the bulk were almost stoichiometric even if after the washing. The absorption edge of AgTaO₃ was around 380 nm in a diffuse reflectance spectrum (Fig. S3†), indicating 3.4 eV of the band gap. Scanning electron microscope observation revealed that the size of AgTaO₃ particles was from several hundreds nm to several μm (Fig. S4†).

Table 1 shows the activities for photocatalytic water splitting over AgTaO₃ loaded with various cocatalysts under UV irradiation. Non-loaded AgTaO₃ produced only a small amount of H₂



Table 1 Photocatalytic water splitting over AgTaO₃ loaded with various cocatalysts under UV irradiation^a

Cocatalyst (wt%)	Loading method	Activity/ $\mu\text{mol h}^{-1}$	
		H ₂	O ₂
None	—	0.5	0
Rh _{0.5} Cr _{1.5} O ₃ (0.05)	Impregnation (623 K - 1 h)	56	28
Rh _{0.5} Cr _{1.5} O ₃ (0.1)	Impregnation (623 K - 1 h)	318	162
Rh _{0.5} Cr _{1.5} O ₃ (0.2)	Impregnation (623 K - 1 h)	400	192
Rh _{0.5} Cr _{1.5} O ₃ (0.3)	Impregnation (623 K - 1 h)	217	111
Cr ₂ O ₃ (0.13)	Impregnation (623 K - 1 h)	1.8	0.9
RuO ₂ (0.2)	Impregnation (673 K - 2 h)	1.6	0.5
NiO (0.2)	Impregnation (543 K - 1 h)	18	4
Pt (0.2)	Photodeposition (<i>in situ</i>)	45	4

^a Photocatalyst: 0.3 g, reactant solution: distilled water (120 mL), cell: top-irradiation cell with a Pyrex window, light source: 300 W Xe-arc lamp ($\lambda > 300$ nm).

without O₂ evolution. In other words, water splitting did not proceed. In contrast, all AgTaO₃ loaded with various cocatalysts produced both H₂ and O₂. However, the amount of evolved H₂ was more than a stoichiometric amount when NiO, RuO₂ and Pt were loaded. When Cr₂O₃ and Rh_{0.5}Cr_{1.5}O₃ were loaded, the stoichiometric amounts of H₂ and O₂ evolved, indicating that ideal water splitting proceeded. In particular, the activity of AgTaO₃ was greatly improved by loading of the Rh_{0.5}Cr_{1.5}O₃ cocatalyst. This result is appropriate because Rh_{0.5}Cr_{1.5}O₃ is known as an effective cocatalyst for photocatalytic water splitting. It is reported that Cr₂O₃ does not work as a cocatalyst for photocatalytic water splitting but Ag coloaded with Cr works as a cocatalyst.²⁵ In the present case, only Cr₂O₃-loaded AgTaO₃ showed the water splitting activity. This is probably because a small amount of metallic Ag still remained on the surface of AgTaO₃ even after washing with an aqueous HNO₃ solution and a Ag–Cr cocatalyst was formed by loading of Cr₂O₃ as an effective cocatalyst. We optimized the loading amount of the Rh_{0.5}Cr_{1.5}O₃ cocatalyst and synthesis conditions of AgTaO₃. The water splitting activity of AgTaO₃ slightly depended on synthesis conditions and 1273 K - 15 h was the best condition for the activity (Table S1†). In addition, the activity was insensitive for addition of an excess amount of Ag. On the other hand, the activity much depended on the loading amount of Rh_{0.5}Cr_{1.5}O₃ cocatalyst and 0.2 wt% was optimum (Table 1). The optimized Rh_{0.5}Cr_{1.5}O₃(0.2 wt%)/AgTaO₃ stably and continuously produced H₂ and O₂ using a Xe lamp (Fig. 1).

Chemical and physical states of the loaded Rh_{0.5}Cr_{1.5}O₃ in Rh_{0.5}Cr_{1.5}O₃(0.2 wt%)/AgTaO₃ before and after water splitting were characterized using a transmission electron microscope (TEM) and an X-ray photoelectron spectroscopy (XPS) because the water splitting activity of AgTaO₃ was greatly improved by loading a Rh_{0.5}Cr_{1.5}O₃ cocatalyst. It was confirmed by TEM that Rh_{0.5}Cr_{1.5}O₃ particles with a diameter of about 10–20 nm were loaded on AgTaO₃ (Fig. 2), as observed for GaN–ZnO.²⁶ In XPS spectra, the binding energy of the Rh 3d_{5/2} peak for Rh_{0.5}Cr_{1.5}O₃(0.2 wt%)/AgTaO₃ was 309.0 eV (Fig. S5†) which is close to not

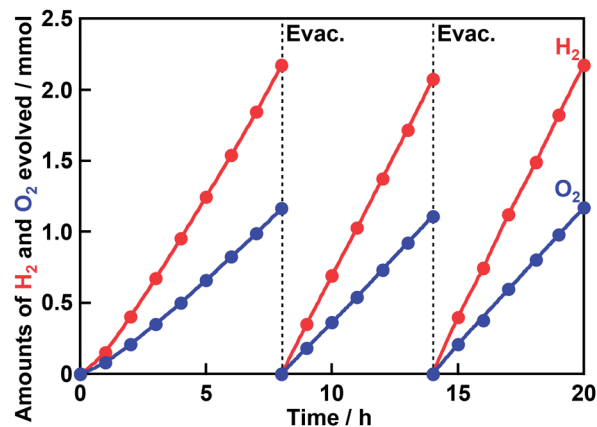


Fig. 1 Photocatalytic water splitting over Rh_{0.5}Cr_{1.5}O₃(0.2 wt%)/AgTaO₃. AgTaO₃ was synthesized by a solid state reaction at 1273 K for 15 h without excess Ag. Rh_{0.5}Cr_{1.5}O₃ was loaded by an impregnation method at 623 K for 1 h. Photocatalyst: 0.3 g, reactant solution: distilled water (120 mL), cell: top-irradiation cell with a Pyrex window, light source: 300 W Xe-arc lamp ($\lambda > 300$ nm).

that for Rh₂O₃ (308.3 eV) but that for Rh_{0.5}Cr_{1.5}O₃ (308.9 eV).²⁶ The slightly positive shift in the binding energy was also observed for the Rh_{0.5}Cr_{1.5}O₃ loaded on GaN–ZnO (309.1 eV).²⁶ These results indicate that the loaded Rh_{0.5}Cr_{1.5}O₃ on AgTaO₃ in the present study was similar to that on GaN–ZnO. Additionally, the TEM image of Rh_{0.5}Cr_{1.5}O₃ cocatalysts did not change so much after photocatalytic water splitting. On the other hand, in the XPS spectra, the Rh 3d_{5/2} peak for Rh_{0.5}Cr_{1.5}O₃(0.2 wt%)/AgTaO₃ after photocatalytic water splitting was broadened to lower binding energy than that before photocatalytic water splitting. This observation indicated that the photocatalyst was activated by partial reduction of Rh in loaded Rh_{0.5}Cr_{1.5}O₃ cocatalyst to the metallic form during the induction period in Fig. 1.

An action spectrum of water splitting on the optimized Rh_{0.5}Cr_{1.5}O₃(0.2 wt%)/AgTaO₃ was measured, as shown in Fig. 3. The maximum AQY was 38% at 340 nm. As far as we know, the AQY is the highest among one-step photoexcitation type water splitting using metal oxide photocatalysts with valence bands consisting of metal cation orbitals. In order to compare the activity of Rh_{0.5}Cr_{1.5}O₃(0.2 wt%)/AgTaO₃ with that

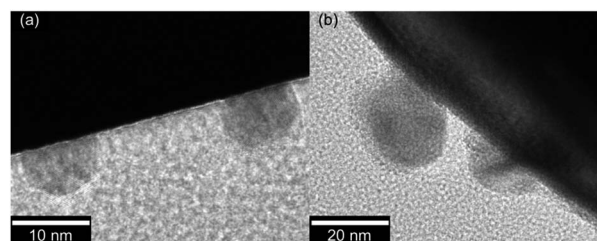


Fig. 2 TEM images of Rh_{0.5}Cr_{1.5}O₃(0.2 wt%)/AgTaO₃ (a) before and (b) after photocatalytic water splitting under UV irradiation using a 300 W Xe-arc lamp. AgTaO₃ was synthesized by a solid state reaction at 1273 K for 15 h without excess Ag. Rh_{0.5}Cr_{1.5}O₃ was loaded by an impregnation method at 623 K for 1 h.



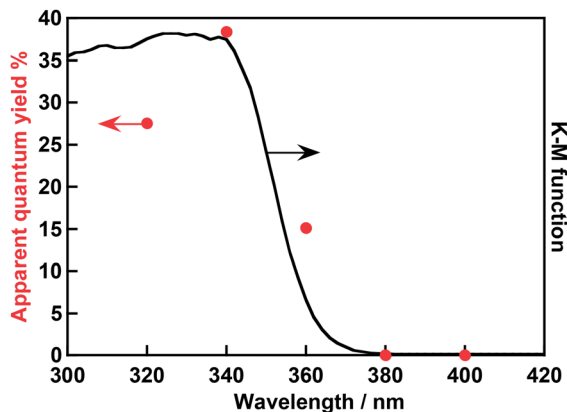


Fig. 3 An action spectrum of water splitting over $\text{Rh}_{0.5}\text{Cr}_{1.5}\text{O}_3(0.2\text{ wt}\%)/\text{AgTaO}_3$ and a diffuse reflectance spectrum of AgTaO_3 prepared by a solid state reaction at 1273 K for 15 h without excess Ag. $\text{Rh}_{0.5}\text{Cr}_{1.5}\text{O}_3$ was loaded by an impregnation method at 623 K for 1 h. Photocatalyst: 0.3 g, reactant solution: distilled water (120 mL), cell: top-irradiation cell with a Pyrex window, light source: 300 W Xe-arc lamp with band-pass filters.

of highly active $\text{NiO}/\text{NaTaO}_3:\text{La}$, photocatalytic water splitting over $\text{Rh}_{0.5}\text{Cr}_{1.5}\text{O}_3(0.2\text{ wt}\%)/\text{AgTaO}_3$ was carried out in an inner-irradiation reaction cell made of quartz equipped with a 400 W high pressure Hg-lamp using 1 g of photocatalyst powder suspended in 340 mL of distilled water, as shown in Fig. 4. Evolution rates of H_2 and O_2 were 20 mmol h^{-1} and 10 mmol h^{-1} , respectively. The activity of $\text{Rh}_{0.5}\text{Cr}_{1.5}\text{O}_3(0.2\text{ wt}\%)/\text{AgTaO}_3$ was similar to that of $\text{NiO}/\text{NaTaO}_3:\text{La}$.¹⁹ This reaction catalytically proceeded because TON was 47. Thus, $\text{Rh}_{0.5}\text{Cr}_{1.5}\text{O}_3(0.2\text{ wt}\%)/\text{AgTaO}_3$ interestingly showed the high activity for water splitting even without doping unlike La-doped NaTaO_3 , Zn, Ca-codoped Ga_2O_3 , and Al-doped SrTiO_3 , suggesting that AgTaO_3 itself has good potential for water splitting. One possible explanation about the potential of AgTaO_3 will be the distortion

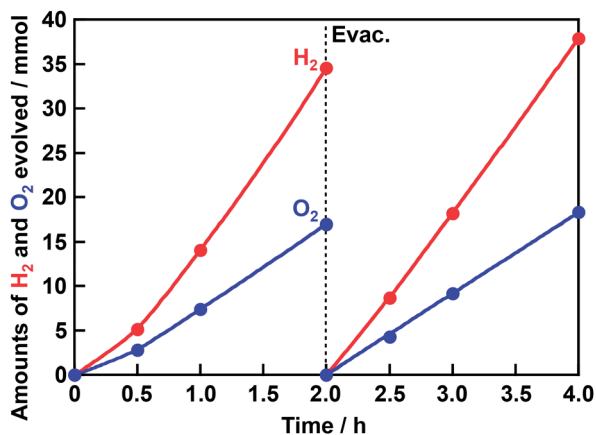


Fig. 4 Photocatalytic water splitting over $\text{Rh}_{0.5}\text{Cr}_{1.5}\text{O}_3(0.2\text{ wt}\%)/\text{AgTaO}_3$ under UV irradiation. Photocatalyst: 1 g, reactant solution: distilled water (340 mL), cell: inner-irradiation cell made of quartz, light source: 400 W high pressure Hg-lamp. AgTaO_3 was synthesized by a solid state reaction at 1273 K for 15 h without excess Ag. $\text{Rh}_{0.5}\text{Cr}_{1.5}\text{O}_3$ was loaded by an impregnation method at 623 K for 1 h.

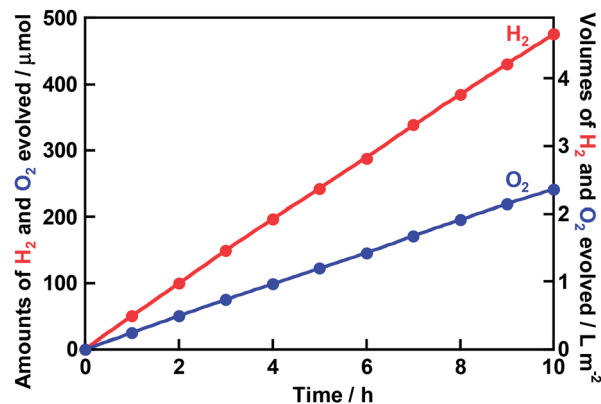


Fig. 5 Photocatalytic solar water splitting over $\text{Rh}_{0.5}\text{Cr}_{1.5}\text{O}_3(0.2\text{ wt}\%)/\text{AgTaO}_3$. AgTaO_3 was synthesized by a solid state reaction at 1273 K for 15 h without excess Ag. $\text{Rh}_{0.5}\text{Cr}_{1.5}\text{O}_3$ was loaded by an impregnation method at 623 K for 1 h. $\text{Rh}_{0.5}\text{Cr}_{1.5}\text{O}_3(0.2\text{ wt}\%)/\text{AgTaO}_3$ was activated by a 300 W Xe-arc lamp in distilled water for 20 h before this reaction (Fig. 1) in order to eliminate the induction period early. Photocatalyst: 0.3 g, reactant solution: distilled water (120 mL), cell: top-irradiation cell with a Pyrex window, light source: a solar simulator with an AM1.5-filter (100 mW cm^{-2}), irradiation area: 25 cm^2 .

of its crystal structure. The Ta–O–Ta bond angle of AgTaO_3 (164 degree) is very similar to that of NaTaO_3 (163 degree).²³ The similarity in the lattice distortion between AgTaO_3 and NaTaO_3 causes a similar property of a conduction band of AgTaO_3 to a highly active NaTaO_3 . Therefore, mobility of photogenerated electrons and a reduction potential of water reduction of AgTaO_3 should be similar to those of NaTaO_3 . Additionally, the valence band of NaTaO_3 is formed by only O 2p orbitals, whereas that of AgTaO_3 is formed by hybridized orbitals between Ag 4d and O 2p.²³ Therefore, photogenerated holes in AgTaO_3 could migrate more easily than those in NaTaO_3 . These positive factors in AgTaO_3 gave high photocatalytic activity.

Water splitting proceeded over the $\text{Rh}_{0.5}\text{Cr}_{1.5}\text{O}_3(0.2\text{ wt}\%)/\text{AgTaO}_3$ photocatalyst even under simulated sunlight irradiation, as shown in Fig. 5. H_2 and O_2 were steadily evolved with the rates of $486\text{ mL m}^{-2}\text{ h}^{-1}$ and $247\text{ mL m}^{-2}\text{ h}^{-1}$, respectively. The STH was estimated to be 0.13%. Additionally, we were able to watch evolved bubbles when $\text{Rh}_{0.5}\text{Cr}_{1.5}\text{O}_3(0.2\text{ wt}\%)/\text{AgTaO}_3$ on the bottom of the reaction cell was irradiated with simulated sunlight under 1 atm at room temperature. The STH of $\text{Rh}_{0.5}\text{Cr}_{1.5}\text{O}_3(0.2\text{ wt}\%)/\text{AgTaO}_3$ is lower than those of $\text{TiO}_2/\text{CoOOH}/\text{RhCrO}_2/\text{SrTiO}_3:\text{Al}$ (STH = 0.4%)²² and $\text{SrTiO}_3:\text{Rh},\text{La-Au-BiVO}_4:\text{Mo}$ photocatalyst sheet (STH = 1.1%),²⁷ whereas it is higher than those of Z-schematic water splitting using $\text{SrTiO}_3:\text{Rh}$ of a H_2 -evolving photocatalyst, BiVO_4 of an O_2 -evolving photocatalyst, and ionic electron mediators such as $\text{Fe}^{3+/2+}$ and $[\text{Co}(\text{bpy})_3]^{3+/2+}$.^{28,29} Thus, we successfully achieved highly efficient one-step photoexcitation type solar water splitting using $\text{Rh}_{0.5}\text{Cr}_{1.5}\text{O}_3(0.2\text{ wt}\%)/\text{AgTaO}_3$ of a valence-band-controlled metal oxide photocatalyst.

Conclusions

$\text{Rh}_{0.5}\text{Cr}_{1.5}\text{O}_3(0.2\text{ wt}\%)-$ loaded AgTaO_3 has arisen as a photocatalyst for solar water splitting in a suspension system. The



AQY of $\text{Rh}_{0.5}\text{Cr}_{1.5}\text{O}_3(0.2 \text{ wt}\%)/\text{AgTaO}_3$ was about 40% at 340 nm. The activity of $\text{Rh}_{0.5}\text{Cr}_{1.5}\text{O}_3(0.2 \text{ wt}\%)/\text{AgTaO}_3$ was similar to that of $\text{NiO}/\text{NaTaO}_3:\text{La}$ under the same experimental condition, using 1 g of photocatalyst powder suspended in 340 mL of distilled water, in an inner-irradiation cell made of quartz equipped with a 400 W high pressure Hg-lamp. AgTaO_3 seems to have good potential for water splitting because $\text{Rh}_{0.5}\text{Cr}_{1.5}\text{O}_3(0.2 \text{ wt}\%)/\text{AgTaO}_3$ showed the high AQY even without doping of elements. $\text{Rh}_{0.5}\text{Cr}_{1.5}\text{O}_3(0.2 \text{ wt}\%)/\text{AgTaO}_3$ also showed the photocatalytic activity for water splitting under simulated sunlight irradiation with the STH of 0.13%. The AQY and STH of $\text{Rh}_{0.5}\text{Cr}_{1.5}\text{O}_3(0.2 \text{ wt}\%)/\text{AgTaO}_3$ were the highest for one-step photoexcitation type water splitting using a valence-band-controlled metal oxide photocatalyst. Thus, it was clarified that a metal oxide photocatalyst with a valence band consisting of metal cation orbitals rather than O 2p could be utilized as a photocatalyst for highly efficient water splitting. The knowledge is expected to be applied to visible-light-driven photocatalysts.

Conflicts of interest

There are no conflicts to declare.

Acknowledgements

This work was supported by JSPS KAKENHI Grant Numbers 17H06433 in Scientific Research on Innovative Areas “Innovations for Light-Energy Conversion (I^4LEC)” and 17H0127. The authors gratefully thank Dr T. Ichihashi for assistance with TEM measurements.

Notes and references

- 1 F. E. Osterloh, *Chem. Mater.*, 2008, **20**, 35–54.
- 2 Y. Inoue, *Energy Environ. Sci.*, 2009, **2**, 364–386.
- 3 A. Kudo and Y. Miseki, *Chem. Soc. Rev.*, 2009, **38**, 253–278.
- 4 R. Abe, *J. Photochem. Photobiol., C*, 2010, **11**, 179–209.
- 5 T. Hisatomi, J. Kubota and K. Domen, *Chem. Soc. Rev.*, 2014, **43**, 7520–7535.
- 6 K. Maeda and K. Domen, *Bull. Chem. Soc. Jpn.*, 2016, **89**, 627–648.
- 7 K. Maeda, T. Takata, M. Hara, N. Saito, Y. Inoue, H. Kobayashi and K. Domen, *J. Am. Chem. Soc.*, 2005, **127**, 8286–8287.
- 8 K. Maeda, K. Teramura, D. Lu, T. Takata, N. Saito, Y. Inoue and K. Domen, *Nature*, 2006, **440**, 295.
- 9 Y. Lee, H. Terashima, Y. Shimodaira, K. Teramura, M. Hara, H. Kobayashi, K. Domen and M. Yashima, *J. Phys. Chem. C*, 2007, **111**, 1042–1048.
- 10 K. Takanebe, T. Uzawa, X. Wang, K. Maeda, M. Katayama, J. Kubota, A. Kudo and K. Domen, *Dalton Trans.*, 2009, 10055–10062.
- 11 C. Pan, T. Takata, M. Nakabayashi, T. Matsumoto, N. Shibata, Y. Ikuhara and K. Domen, *Angew. Chem., Int. Ed.*, 2015, **54**, 2955–2959.
- 12 C. Pan, T. Takata and K. Domen, *Chem.–Eur. J.*, 2016, **22**, 1854–1862.
- 13 C. Pan, T. Takata, K. Kumamoto, T. Minegishi, M. Nakabayashi, T. Matsumoto, N. Shibata, Y. Ikuhara and K. Domen, *J. Mater. Chem. A*, 2016, **4**, 4544–4552.
- 14 K. Maeda, D. Lu and K. Domen, *Chem.–Eur. J.*, 2013, **19**, 4986–4991.
- 15 J. Xu, C. Pan, T. Takata and K. Domen, *Chem. Commun.*, 2015, **51**, 7191–7194.
- 16 Z. Wang, Y. Inoue, T. Hisatomi, R. Ishikawa, Q. Wang, T. Takata, S. Chen, N. Shibata, Y. Ikuhara and K. Domen, *Nat. Catal.*, 2018, **1**, 756–763.
- 17 Q. Wang, M. Nakabayashi, T. Hisatomi, S. Sun, S. Akiyama, Z. Wang, Z. Pan, X. Xiao, T. Watanabe, T. Yamada, N. Shibata, T. Takata and K. Domen, *Nat. Mater.*, 2019, **18**, 827–832.
- 18 R. Asai, H. Nemoto, Q. Jia, K. Saito, A. Iwase and A. Kudo, *Chem. Commun.*, 2014, **50**, 2543–2546.
- 19 H. Kato, K. Asakura and A. Kudo, *J. Am. Chem. Soc.*, 2003, **125**, 3082–3089.
- 20 Y. Sakata, T. Hayashi, R. Yasunaga, N. Yanaga and H. Imamura, *Chem. Commun.*, 2015, **51**, 12935–12938.
- 21 H. T. Chiang, H. Lyu, T. Hisatomi, Y. Goto, T. Takata, M. Katayama, T. Minegishi and K. Domen, *ACS Catal.*, 2018, **8**, 2782–2788.
- 22 H. Lyu, T. Hisatomi, Y. Goto, M. Yoshida, T. Higashi, M. Katayama, T. Takata, T. Minegishi, H. Nishiyama, T. Yamada, Y. Sakata, K. Asakura and K. Domen, *Chem. Sci.*, 2019, **10**, 3196–3201.
- 23 H. Kato, H. Kobayashi and A. Kudo, *J. Phys. Chem. B*, 2002, **106**, 12441–12447.
- 24 Y. Inoue, *Energy Environ. Sci.*, 2009, **2**, 364–386.
- 25 K. Maeda, K. Teramura, N. Saito, Y. Inoue and K. Domen, *J. Catal.*, 2006, **243**, 303–308.
- 26 K. Maeda, K. Teramura, D. Lu, T. Takata, N. Saito, Y. Inoue and K. Domen, *J. Phys. Chem. B*, 2006, **110**, 13753–13758.
- 27 Q. Wang, T. Hisatomi, Q. Jia, H. Tokudome, M. Zhong, C. Wang, Z. Pan, T. Takata, M. Nakabayashi, N. Shibata, Y. Li, I. D. Sharp, A. Kudo, T. Yamada and K. Domen, *Nat. Mater.*, 2016, **15**, 611–615.
- 28 Y. Sasaki, H. Kato and A. Kudo, *J. Am. Chem. Soc.*, 2013, **135**, 5441–5449.
- 29 H. Kato, Y. Sasaki, N. Shirakura and A. Kudo, *J. Mater. Chem. A*, 2013, **1**, 12327–12333.

